Separation and Purification Technology 318 (2023) 123943

Contents lists available at ScienceDirect

Separation and Purification Technology

journal homepage: www.elsevier.com/locate/seppur

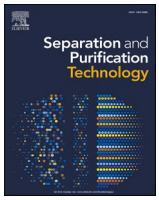

Willow bark proanthocyanidins with potential for water treatment: Chemical characterization and zinc/bisphenol A removal

Dou Jinze [a,*], Varila Toni [b,e], Salminen Juha-Pekka [c], Tuomikoski Sari [b], Hietala Sami [d], Hemmi Maria [c], Hu Tao [b], Lassi Ulla [b,e], Vuorinen Tapani [a]

[a] Department of Bioproducts and Biosystems, Aalto University, Espoo, Finland
[b] Research Unit of Sustainable Chemistry, University of Oulu, Oulu, Finland
[c] Natural Chemistry Research Group, Department of Chemistry, University of Turku, Turku, Finland
[d] Department of Chemistry, University of Helsinki, Helsinki, Finland
[e] Kokkola University Consortium Chydenius, University of Jyväskylä, Kokkola, Finland

ARTICLE INFO

Keywords:
Proanthocyanidins
Procyanidins
Prodelphinidins
Tannin
NMR
UPLC-MS/MS
Water treatment

ABSTRACT

This study investigates the chemical structure of proanthocyanidin-rich crude extracts from willow bark and these materials were tested initially as adsorbents for artificial (waste)water treatment. The crude extracts were obtained through mild water extraction and the colorant fractions were further chromatographically fractionated to understand the chemical structure of the willow bark proanthocyanidins. The chemistry of crude extracts and purified fractions were investigated using nuclear magnetic resonance (NMR) and ultraperformance liquid chromatography-tandem mass spectrometry (UPLC-MS/MS). Both NMR (liquid and solid-state) and UPLC-MS/MS suggest that the crude extracts constitute of interflavan linked flavan-3-ols, i.e. proanthocyanidins with both procyanidin (PC)-type and prodelphinidin (PD)-type subunits, with the PC/PD ratio of approximately 2.3–2.5. PD-type proanthocyanidins were detected from the purified colorant fractions only with UPLC-MS/MS. Both the UPLC-MS/MS and size exclusion chromatography suggest that the crude extracts have an average oligomerization degree of roughly 5–6 flavan-3-ol units. Adsorption experiments showed that the activated foams made of crude extracts were effective in removing both zinc and Bisphenol A (BPA) with removal efficiencies of roughly 80–90% and thus these willow bark-derived proanthocyanidins are promising in water treatment. The significance of this study suggests the upgrading use of crude extracts for water treatment could significantly improve the value of willow bark.

1. Introduction

The first step in using roundwood trees to produce pulp and timber is to remove the bark, which has been a long tradition in the forest industry for decades. Extensive research has focused on the valorizations of the wood components such as cellulose and lignin, but almost exclusively in those of the matrix of wood. [1] However, wood bark with estimated annual turnover of 359 million m^3 world-wide [2] accounts for about 10–15 % of the volume of a typical wood log material turnover. Often the bark is only used for energy production for the pulp mill or sawmill and thus remains by far the largest underutilized biomass resource on the earth. Unlike the main polymeric components in matrix wood, i.e. cellulose, hemicellulose, and lignin, wood bark mainly consists of tannin-rich extractives, pectin, suberin, and starch. This makes valorization of the wood bark challenging as the bark has also a rather heterogeneous composition morphologically. Because of this complexity, attention is currently paid on solvent-extractable fractions of the bark [3,4]. Furthermore, the extractable fractions do not represent the main bulk mass of the bark and thus do not significantly influence the overall energy value of the bark and can be removed without too negatively affecting the energy balance of the mill.

Tannins are complex polyphenolic biomolecules constituted of three major groups: hydrolysable tannins (HTs), proanthocyanidins (PAs) and phlorotannins. [5,6] Of these, phlorotannins are mainly found in marine organisms such as brown algae, while HTs and PAs are widely present in trees and their bark as well. These two tannin groups have significant differences in both their structures and evolutionary history. Gymnosperms can only produce PAs, but no HTs, while many angiosperms can

* Corresponding author.
E-mail address: jinze.dou@aalto.fi (D. Jinze).

https://doi.org/10.1016/j.seppur.2023.123943
Received 30 January 2023; Received in revised form 29 March 2023; Accepted 23 April 2023
Available online 28 April 2023

produce both. HTs are esters of a polyol and gallic acid residues with considerable modifications taking place via oxidative and oligomerization processes, reaching all the way to even 8624 Da sizes. PAs are oligomers and polymers of flavan-3-ol units, with as shown e.g. in procyanidins (PCs) and prodelphinidins (PDs) (Fig. 1**c**). In many cases, plant PAs are a combination of PC and PD units in same molecules, with hundreds of different oligomers and polymers typically present in the same plant species. [5,6] Particularly the tannin fractions from bark of softwood trees, e.g., spruce [7] and pine [8], have been studied. They are reported as adsorbents (or biocoagulant) for removal of metal ions from industrial wastewater due to their non-toxic natural polyphenolic nature with abundant number of adjacent hydroxyl groups. [9,10] There are also applications of utilizing bark tannin as a substitute to phenols for adhesive applications. [11]

Short-rotation willow has been studied mainly as an energy resource in the last decades globally. Cultivated willow is a short-rotation woody crop that can germinate and develop effectively for example in discarded peatlands and other low-nutrient soils. Its growth requires only moist soil, and it is insensitive to soil quality (sandy or clay) and pH. [12] Willow trees are harvested in a cycle of two to four years, seeding cuttings are usually planted as 20 cm long cuttings at a density of 10,000 cuts/ha. In southern Sweden, productivity of willow has been reported up to > 30 ton/ha and the willow plantations were reported to be approximately 17,000 ha [13] in the whole of Sweden between 1991 and 1996. This means roughly 0.1 million tons of willow bark available each year. As the willow bark contains high value metabolites (e.g. for pharmaceutical or medical uses) [14,15] and functional fiber bundles (e.g. as antibacterial materials) [16], the value from the bark can be theoretically multi-fold in comparison with the value of wood if the wood and bark be utilized separately [17]. Debarking of willow can also substantially enhance the efficiency of acetone–butanol–ethanol (ABE) fermentation from willow. [18] The long-underappreciated willow bark residue may be upgraded from an energy source into high-value fiber and proanthocyanidins-enriched biochemicals.

Increasing industrial activities and technological developments have led to the release of larger number of metals into the environment. Because of the toxic effects of the presence of heavy metals and their accumulation through the food chain, contamination of water environments is a worldwide environmental problem. Although small quantities of heavy metals are essential for the growth of living organisms, excessive levels may lead to damage and their accumulation over time may subsequently pose health threats also for humans. For example, acute toxicity of zinc may lead to throat dryness and cough weakness and may ultimately leads to human epidemics. [19] Many plastics and resin materials contain Bisphenol A (BPA) and it has also been detected in municipal wastewater. BPA enter the environment in a concentration that may pose a risk to human health [20,21]. Traditionally, heavy metals and BPA can be reduced by chemical precipitation, ion exchange, or ultrafiltration ect. However, these methods are often either expensive or their manufacturing process is not sustainable. [22] Therefore, the search of more bio-based adsorbents for water treatment have drawn attention.

Preparative chromatography has been demonstrated effective for purifying both high molecular weight colorant fractions and small molecular weight fractions (e.g. picein and triandrin) from willow bark water extracts. [23] As the colorants elute separately from other small Mw aromatic compounds (**Fig. S1, Table S1-S2**) from the column, we were inspired to elucidate the chemical profile behind the purified colorant fraction. Separation of the conjugated tannin chromophores from aqueous extracts of willow bark could also reveal their full potential as a bioadsorbent for wastewater treatment. A lot of studies have been conducted on the crude extracts of willow bark, especially the small Mw components, [14,24,25] but there is not much scientific data on the chemistry of high Mw proanthocyanidins from willow bark. In this paper we utilize a combination of UPLC-MS/MS, NMR spectroscopy and size exclusion chromatography (SEC) to elucidate the chemical structure of the crude extracts and its purified fractions of polyphenol colorants, and to explore further this fraction of proanthocyanidins as a source for water treatment. The efficiency of water treatment was initially studied through adsorption experiments towards zinc and BPA.

2. Materials and methods

2.1. Materials and chemicals

Two-year-old willow hybrid Klara was harvested from the plantation of Carbons Finland Oy (Kouvola, Finland) on 5 May 2019. Four-year-old willow hybrid Karin was sampled from a trial field belonging to VTT Technical Research Centre of Finland Ltd (Kyyjärvi, Finland) on October 17, 2014. Willow hybrids "Karin" and "Klara" have been selected for this study because of its most characteristic features of abundant extractives and the relatively long and thick-walled fibers. [14,16,17,18,23] Willow bark was manually peeled from willow biomass. The oven-dried (50 °C) willow bark was further Wiley-milled (<1mm mesh size) and stored at −20 °C freezer before further use. Acetone, acetonitrile, arabinose, acetone-d_6, (+)-catechin, D_2O, (−)-epicatechin, (−)-epigallocatechin, fructose, galactose, (−)-gallocatechin, glucose, procyanidin B1, rhamnose, and xylose were all analytical grade and supplied from Sigma-Aldrich, Finland. Furfural alcohol (98%) and Tween 85 were acquired from Acros Organics, Finland. *p*-toluenesulfonic acid monohydrate (PTSA, 99%) and *n*-pentane (99.4%) were supplied from Merck KGaA.

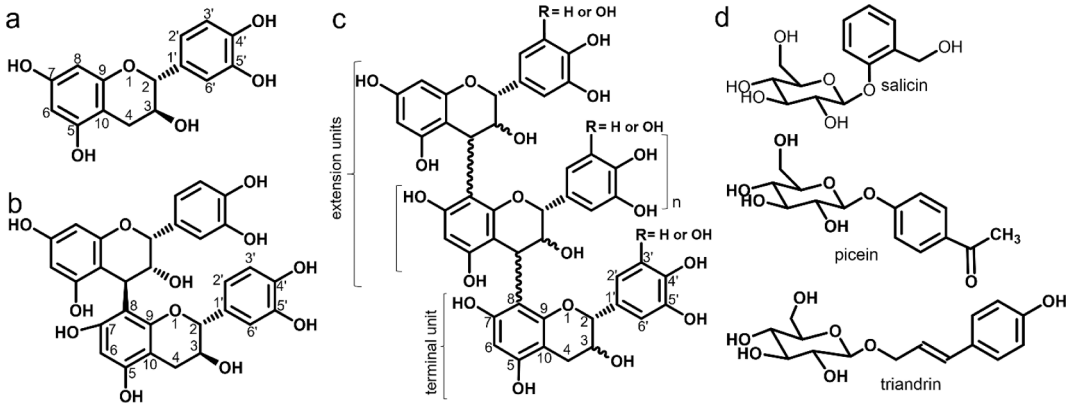

Fig. 1. Generic repeating unit of proanthocyanidin (PA) tannin and other small molecular weight (Mw) aromatic compounds from crude extracts of bark from willow hybrid Karin. a (+)-Catechin (CAS 154–23-4). b Procyanidin B1 (20315–25-7). c Flavan-3-ol subunits (R = H, catechin or epicatechin are in procyanidins (PC) form; R = OH, gallocatechin or epigallocatechin are in prodelphinidins (PD) form). [5,6] d Small Mw aromatics (picein, salicin, and triandrin).

2.2. Experimental flow

2.2.1. Chromatographic purification of the colored fractions

Peeled willow bark was first extracted with water at temperature of 80 °C within 20 mins according to the optimized condition published previously. [14] Then the non-soluble residues were filtered using the qualitative filter paper (12–15 μm, VWR) by vacuum filtration. The crude extracts were then finally freeze dried and stored in the amber glass bottles for further chemical characterization and adsorption experiments. Analysis of the colored fractions of the willow bark crude extracts are essential to provide knowledge for understanding the chemistry of proanthocyanidins. The main recovery steps (Fig. 2) were implemented with preparative-scale chromatography, [23] which separates the targeted compounds depending on their molecular size and hydrophobicity. PF0 (7 w/w, %) and PF1 were separated from crude extracts (100 w/w, %) by CA 10GC, PF 1–1 (3 w/w, %) and PF 1–2 (4 w/w, %) were further purified from fraction PF1 by Sephadex G-10 as the stationary phase. The estimated mass balance of the purified fraction and fractionation cut points are shown in Fig. 1 and fully summarized in **Fig. S1** and **Table S1–S2**.

2.2.2. Foam and activated carbon preparation

For the adsorption studies the samples were formulated to foams. Briefly, crude extracts were mixed with deionized water, furfural alcohol, and surfactant Tween 85 in a glass beaker, then the mixture was blended mechanically for 5–10 min. Pentane (the blowing agent) and PTSA (65% solution, acid catalyst) were then introduced to the homogenized mixture and blended for another 10 s. Foam formed immediately once the beaker was placed in an oven at 100 °C and hardened when kept at 100 °C for a further 24 h. Finally, the hardened foam was crushed and placed inside a section of stainless-steel pipe and then steam-activated in a tubular fixed-bed reactor. The temperature was increased from 20 °C to 800 °C using a 5 °C/min ramp. At the target temperature, steam activation was carried out by injecting water at velocity of 0.5 mL/min for 3 h to the reactor. Nitrogen was flushed into the reactor at velocity of 10 mL/min during the whole activation to avoid sample's oxidation. The morphological structure of the produced foam and activated foam were imaged using a Zeiss ULTRA plus field emission scanning electron microscopy. The yields after the activations for Klara hybrid was 38.7% and for Karin hybrid it was 36.7% compared to starting mass of crude foam. Detailed amounts of the components to obtain the crude foam were outlined in **Table S3**.

2.2.3. Specific surface area, pore volume, and pore size distribution

Nitrogen adsorption–desorption isotherms were obtained to characterize the specific surface area and pore size distribution using Micromeritics ASAP 2020 instrument (Micromeritics Instrument, Norcross, USA). Roughly 150 mg sample was degassed under low pressure (2 mmHg) at 140 °C for two hours. Adsorption isotherms were obtained by submerging the sample tubes under liquid nitrogen to achieve isothermal state followed by purging with gaseous nitrogen. BET (Brunauer–Emmett–Teller) method [26] was used to calculate the specific surface areas. Assuming the pore size is slit-formed, the calculation of pore size distribution (PSD) of pore volumes (vol %) followed the individual pore size (micro-, meso-, and macro-) volumes with NLDFT model [27,28]. Micro-pores as small as 1.5 nm in diameter could be identified. The specific surface area can be measured with a precision of 5 % based on a previous study. [29]

2.2.4. Batch adsorption experiments

The adsorption capacity towards BPA and zinc was studied by batch adsorption. Raw materials (Karin and Klara willow bark), foam samples (Ka-F and Kl-F) and activated foams (Ka-A-F and Kl-A-F) were investigated. Samples were sieved to under 150 μm particle size. Experiments were made at pH 6 using initial adsorbate concentration of 50 mg/L, 24 h adsorption time and adsorbent dosage of 5 g/L. Volume of the batch was 25 mL. Laboratory shaker with 300 rpm was implemented to mix adsorbent and adsorbate. All adsorption experiments were conducted in duplicate. Samples were filtered through 0.45 μm filter paper (Sartorium Stedim Biotech) after 24-hour adsorption.

2.3. Characterization

2.3.1. SEC of proanthocyanidin

SEC experiments for both the crude extracts and the purified colorant fractions were carried out with an Agilent 1260 Infinity II Multi-Detector GPC/SEC System including a UV detector. Three Waters 7.8 mm × 300 mm Ultrahydrogel columns (500 Å, 250 Å, and 120 Å) with a 6 mm × 40 mm Ultrahydrogel guard column were implemented with the flow rate of 0.5 mL/min using 0.1 M $NaNO_3$ as the eluent. The injection volume was 100 μl. For molar mass determination, the columns were calibrated using narrow-polystyrene sulfonate (PSS) standards under the 280 nm UV absorbance.

2.3.2. Liquid-state (^{13}C and HSQC) NMR of proanthocyanidin

Liquid-state NMR spectroscopy was applied for analyses of the

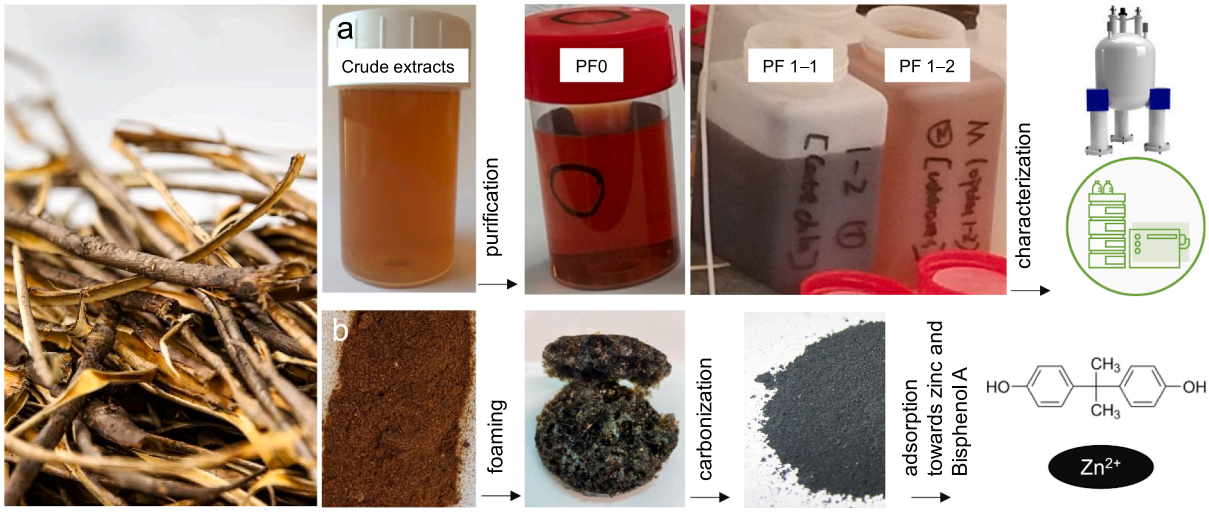

Fig. 2. Experimental flow of chromatographic purification, chemical characterization, and adsorption for the crude extracts (100 w/w, %) of willow bark. a Chemical elucidation of the produced colorant fractions PF0 (7 w/w, %), PF 1–1 (3 w/w, %), and PF 1–2 (4 w/w, %). [23] b Raw powdered crude extracts were foamed, carbonized, and activated, and the adsorption capacities towards zinc and BPA were studied.

chemical structures of crude extracts and purified fractions. Measurements were performed using a 400 MHz Bruker Avance III spectrometer. Acetone-d_6: D_2O (v:v; 1:1) (δC/δH, 29.92/2.05 ppm) was used not only as the internal reference for the chemical shift calibration but also as the deuterated solvent to dissolve the sample. [30] ^{13}C spectra were measured at room temperature with a relaxation delay of 2 s with 18 K scans and 2D HSQC was performed to correlate the proton and carbon shifts.

2.3.3. Solid-state NMR of proanthocyanidin

Solid-state ^{13}C CPMAS NMR spectra were acquired by employing a double resonance CPMAS probehead. The ground samples were packed into 4 mm outer diameter ZrO2 rotors, sealed with KEL-F endcaps and spun at spinning frequency of 8 kHz. ^{13}C CPMAS spectra were obtained at room temperature with at least 3000 scans using a 5 s relaxation delay and 1 ms contact time for cross polarization. The spectra were externally referenced to adamantane [31].

2.3.4. UPLC-MS/MS of proanthocyanidin

Dried samples were dissolved in 10% aq. acetonitrile (final concentration 2 mg/mL), filtered with 0.20 μm polytetrafluoroethylene (PTFE) filters, and analysed with UHPLC-MS/MS as outlined previously [32,33]. Procyanidin (PC) and prodelphinidin (PD) subunits (both terminal and extension units) of oligomeric and polymeric proanthocyanidins (PA) were detected by the PC- and PD-specific group-specific MS/MS tools to allow the calculation of total PA content of the analysed sample in mg/g dry weight, the PC and PD share, and the mean degree of polymerization (mDP) of PAs present in samples analysed based on two or three independent measurements. Previously purified and well characterized PC-rich and PD-rich PA-fractions [32] were used as external standards for both PC and PD quantitation and for the calibration of the mDP.

2.3.5. HPLC/UV–vis of foam and activated carbon

Zinc concentration was determined using atomic absorption spectroscopy (PerkinElmer A Analyst 200, Waltham, MA, USA). BPA concentration was quantified using high-pressure liquid chromatography (HPLC) at 226 nm wavelength with ultraviolet–visible (UV–vis) detectors (Shimadzu SPD-10 A).

2.3.6. FESEM of foam and activated carbon

The microstructure shown in FESEM images were obtained using a Zeiss Sigma field emission scanning electron microscope (FESEM, Carl Zeiss Microscopy GmbH, Jena, Germany) at an accelerating voltage of 5 kV.

2.4. Calculation

The adsorption capacity, q:

$$q = \frac{(C_0 - C_e) \times V}{m} \quad (1)$$

where C_0 refers to the initial concentration of adsorbate (mg/L), C_e refers to the equilibrium concentration of adsorbate (mg/L), V is the volume of solution (L) and m is the adsorbent mass (g).

3. Results & discussion

3.1. Mass balance and chromatographic purification

Crude water extracts represent approximately 20 (w/w, %) of the bark from *Salix* (Klara and Karin) hybrids. [34] Table 1 displays the mass balance of the crude extracts from bark of both Klara and Karin willow hybrids. The main identified phenolic compounds are salicin, catechin, epicatechin, and triandrin. [34] The Stiasny number reaction was adopted to determine the tannin reactivity of the crude extracts towards formaldehyde. [35] The determined reactive tannin was 56 (w/w, %) in Karin bark. The identified phenol represents only 6.6 (w/w, %) and 15.5 (w/w, %) from crude extracts of bark from Karin and Klara, respectively, indicating the rest of formaldehyde-reacting phenol could possibly originate from the unreacted proanthocyanidins (approximately 49.5 (w/w, %), Table 1) that are present largely at the crude extracts of the willow hybrid Karin bark.

Table 1
Mass balance of the water extracts (mg/g crude extracts) [34] from willow bark Karin and Klara. Overall determined phenolics refer to the sum of catechin, epicatechin, and triandrin. "a" denotes that the proanthocyanidins (w/w %) = overall reactive tannin (w/w %) – overall determined phenolics (w/w %). All the measurements were performed two times and the standard deviation are included inside the parenthesis.

Component mg/g	Karin	Klara
Salicin	1 (0.2)	7 (0.02)
Picein	51 (2)	0.1 (0.1)
Catechin	19 (1)	21 (0.01)
(-)-Epicatechin	0.2 (0.1)	0.1 (0.03)
Triandrin	45 (1)	127 (0.3)
Raffinose	1 (0.1)	31 (0.5)
Monosaccharides (Glc + Fru)	144 (2)	149 (0.1)
Sucrose	1 (1)	45 (0.6)
Overall identified	262	380
Overall phenol (low Mw)	66	155
Overall reactive tannin	560	n.d.
Proanthocyanidins[a]	495	n.d.

To improve the understanding of the composition of the high Mw proanthocyanidin, the crude extract was fractionated by stationary phases of CA-10GC and Sephadex G10. The resulting multiple colorant tannin fractions were purified from the crude extracts using the column chromatography. [23] The Mw of each purified fraction was measured by SEC (**Fig. S2** and **Table S4**). The average degree of oligomerization of the crude extracts was 5–6 flavan-3-ol units. It has been reported that 70% ethanol extract of *Salix* purpurea L. bark contains up to 3-unit flavan-3-ol oligomers [36], including derivatives formed from reactions with other phenolic compounds. The flavan-3-ols obtained were catechin, epicatechin, gallocatechin, and catechin-3-O-(1-hydroxy-6-oxo-2-cyclohexene-1-carboxylic acid)-ester.

3.2. NMR characterization

Solid state ^{13}C NMR is a valuable tool for in-situ characterization of proanthocyanidin tannins. The solid-state NMR spectra of the purified fractions (PF0, PF 1–1, and PF 1–2), crude extracts, and Karin bark are shown in Fig. 3. The overlap resonances especially between the willow bark (Fig. 3**a**) and crude extracts (Fig. 3**b**) indicate interferences from components like lignin, pectin and holocellulose. [37,38] Characteristic distinctive resonances at 155 ppm (non-protonated C5, C7, and C8a, Fig. 1), 145 ppm (non-protonated C3′, C4′, and C5′), and 132 ppm (non-protonated C1′) were observed in the spectra of crude extracts and its purified fractions (PF0, PF 1–1, and PF 1–2). [35,37,38] The distinctive features of procyanidins (PCs) and prodelphinidins (PDs) units can't be distinguished from solid-state NMR.

The liquid-state ^{13}C NMR spectra are shown in Fig. 4. Inspection of the liquid state NMR spectra and comparison with the published data [30,39,40] show typical signals attributed to procyanidin (PC) and prodelphinidin (PD) units. The signal centered at 145.0 ppm and 145.1 ppm (Fig. 4) can be identified to C3′ and C4′ in the B-ring of the flavan-3-ol units in PC form, respectively. Typical chemical characteristic signals for C3′ and C5′ (centered 145.9 ppm) of the PD units are also seen in ^{13}C NMR, Fig. 4. The remaining specific aromatic resonances show the 116.2 ppm and 119.8 ppm for the C2′ (or C5′) and C6′, respectively. The signals at 131.7 (C-1), 77.2 (C-2, cis form), 70.7 (C-3, extender part), and 67.5 (C-3, terminal part) ppm can be assigned to the attached flavan-3-ol units (Fig. 1). The peaks that are shown between the region 90–110 ppm

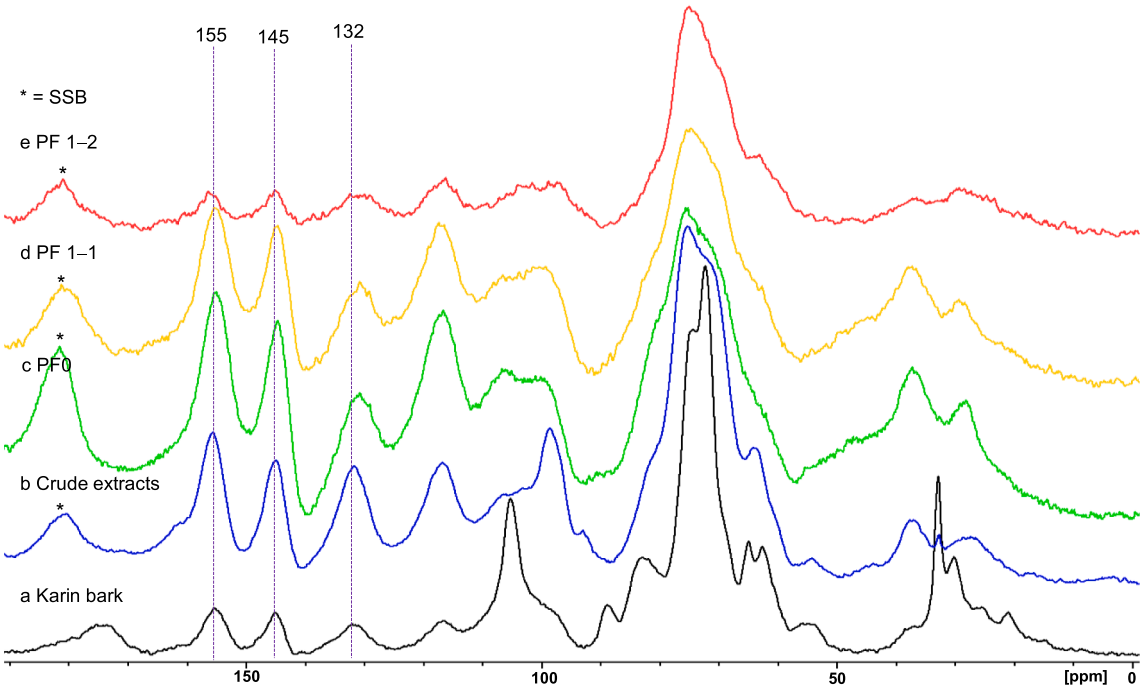

Fig. 3. Solid state CPMAS NMR spectrum of the purified polyflavonoid tannin fractions in comparison with the original Karin bark and its crude extracts. a Karin bark. b Crude extracts. c PF0. d PF 1–1. e PF 1–2.

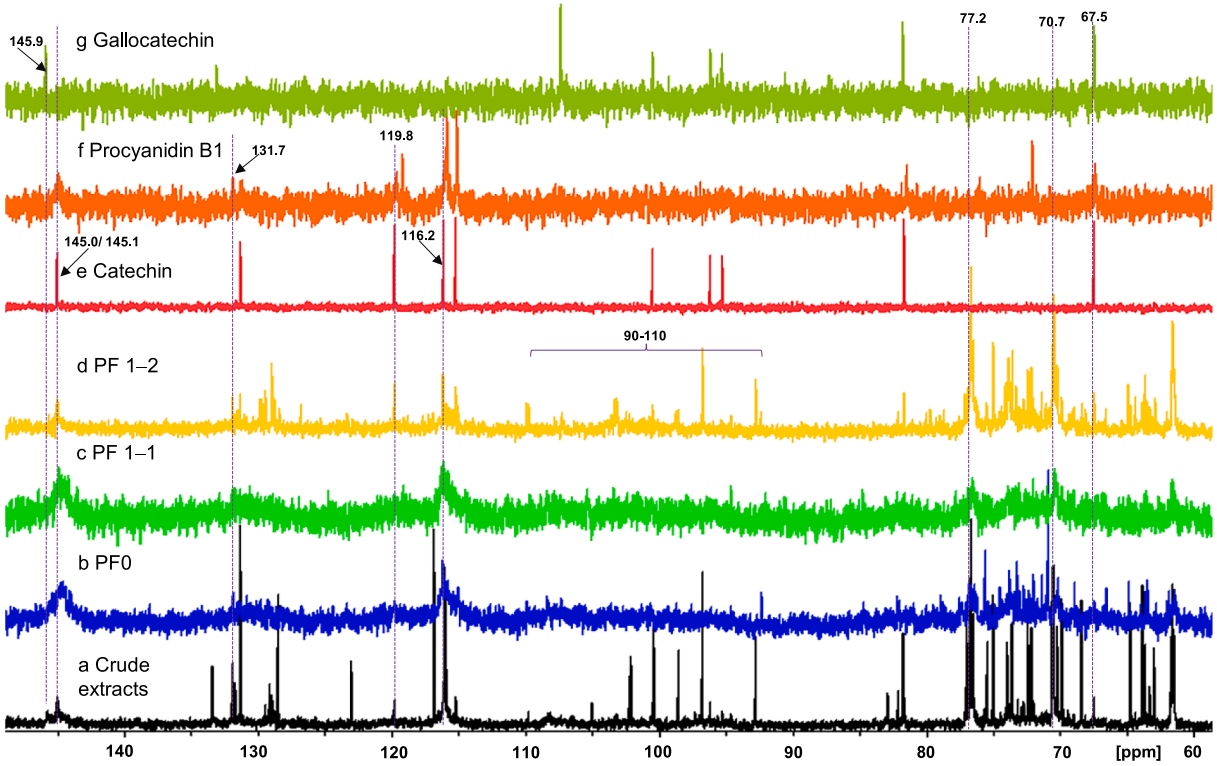

Fig. 4. Room temperature ^{13}C NMR spectrum of both the crude extracts and its purified fractions from willow Karin bark in solvent of acetone-d_6: D_2O (v:v; 1:1) in comparison to the authentic compounds of catechin and procyanidin B1. a Crude extracts. b PF0. c PF 1–1. d PF 1–2. e Authentic (+)-catechin. f Authentic procyanidin B1. For labelling see Fig. 1. Estimated integral ratio of PC-unit (C3′ and C4′, 1)/ PD-unit (C3′ and C5′, 0.4344) of the crude extracts = 2.3.

was sensitive to the units (C2′, C6′, C6, C8, and C10) in both form of PC and PD. The HSQC spectrum at Fig. 5, confirms the structure characteristics of PC and PD form based on literature [37,41,42] and model compounds catechin, gallocatechin, and procyanidin B1. The peaks at δC/δH 115.03/6.86 (B ring-2′), 115.53/6.68 (B ring-5′) and 119.08/6.62 (B ring-6′) represent the correlations of the protonated PC form. Green triangle (Fig. 5) highlights the assignment of the characteristic peaks of the C/H-2′,6′ (δC/δH, 105–110/6.4–6.8 ppm) of the protonated

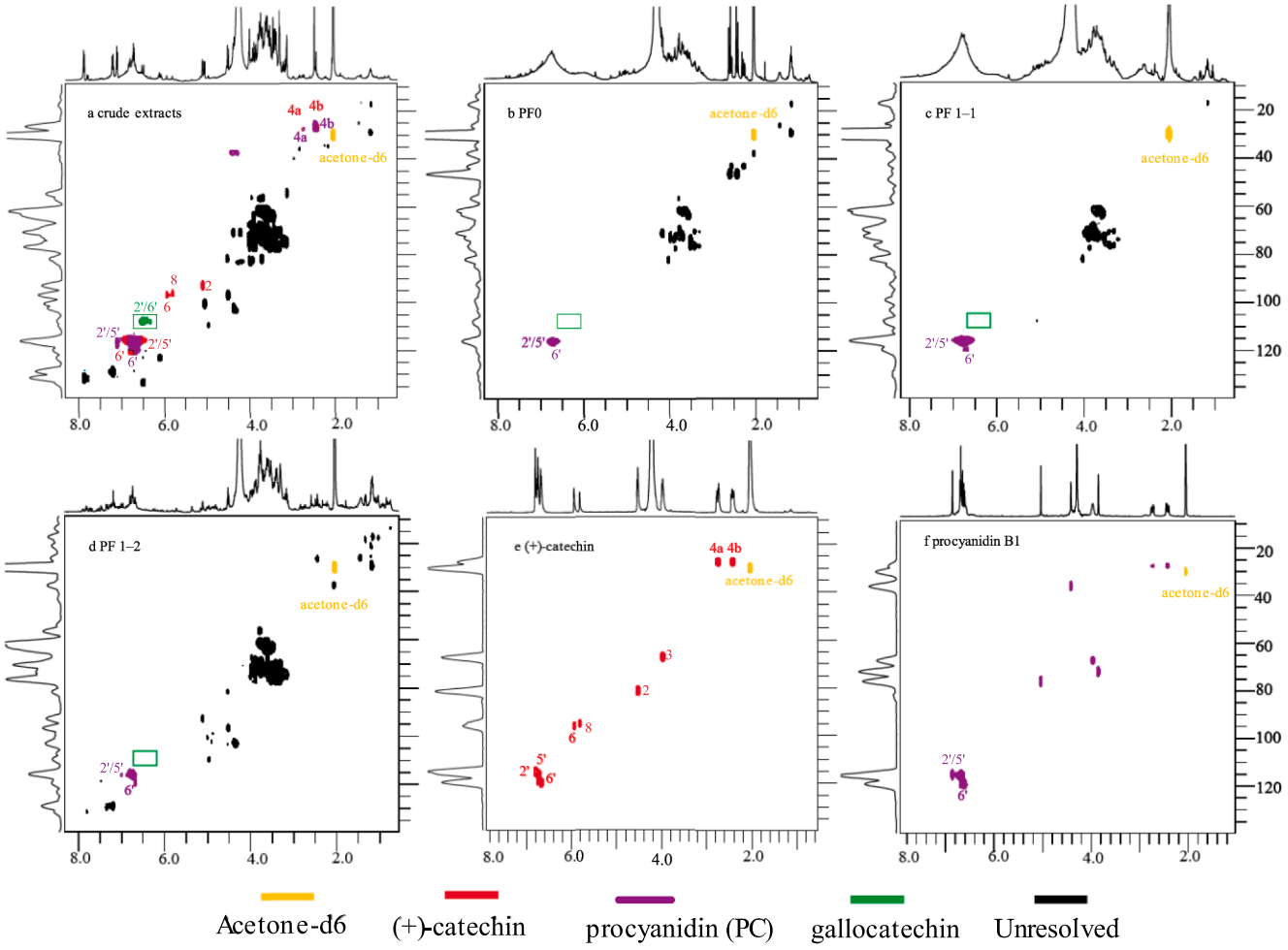

Fig. 5. HSQC NMR spectrum of both the crude extracts and fractions from Karin bark in solvent of acetone-d_6: D_2O (v:v; 1:1) in comparison to the authentic compounds of catechin, gallocatechin, and procyanidin B1. a Crude extracts. b PF0. c PF 1–1. d PF 1–2. e Authentic (+)-catechin (for labelling see Fig. 1). f Authentic procyanidin B1. HSQC NMR spectrum of epicatechin, gallocatechin, and epigallocatechin are shown in **Fig. S4-S6**. Estimated volume integral ratio of PC-unit (C2′ and C5′)/ PD-unit (C2′ and C6′) from crude extracts = 2.3.

prodelphinidin (PD) units and they were both identified from the crude extracts. ^{13}C NMR spectrum of the fraction PF 1–2 contained several overlapped signals at chemical shifts of polymeric tannins from leaves of *Leucaena leucocephala* hybrid Rendang in D_2O/acetone-d_6 (v:v; 1:1) (**Fig. S3**) [30]. Only procyanidin (PC) form was identified from its purified polyflavonoid tannins (i.e. PF0, PF 1–1, and PF 1–2). This is possibly because ^{13}C measurement parameters (such as relaxation delay) were not optimized for the purified fractions so that prodelphinidin (PD) units may be filtered out.

3.3. UPLC-MS/MS characterization

UPLC-MS/MS analyses were performed to further support compound identifications. The PCs and PDs can be detected and quantified using group-specific 2D fingerprint method. [33] This method relies on the fragmentation of oligomeric and polymeric PAs in the MS ion source by using a cone voltage much higher than used for the analysis of individual flavan-3-ols such as catechin and gallocatechin. The fragments thus represent the PC and PD units originally bound to the oligomeric and polymeric PAs and are detected by MS/MS methods specific to both terminal and extension units of the PCs and PDs. The use of a small cone voltage revealed sharp peaks presenting gallocatechin and epigallocatechin (Fig. 6**e**) together with catechin and epicatechin (Fig. 6**i**) monomers. The PD-containing PA oligomers showed as peaks with higher cone voltages in Fig. 6 b->d and the PC-containing PA oligomers in Fig. 6 h->g. These same chromatograms also displayed the smaller polymeric PD- and PC-containing PAs as the chromatographic humps eluting after the oligomeric peaks. Finally, the largest PD-containing polymeric PAs showed with the highest cone voltage used in the chromatogram 6b, and the largest PD-containing polymeric PAs in the chromatogram 6f. The gradual detection of larger and larger PAs with increasing cone voltage was evident also from the chromatograms as the PC and PD hump shifted to the right as the method fragments and thus detects bigger and bigger PAs from Fig. 6 d->b and Fig. 6h->f. The detection of PD was very low at samples PF 1–1 and PF 1–2, i.e. close to the baseline noise, as the hump was barely visible even with this sensitive detection method (Fig. 6**b**).

According to the identification protocol [33], the total content of proanthocyanidins, PC and PD, and mDP were reported in Table 2. Unlike the NMR results, prodelphinidins (PD) – units were also detected from PF0 although their presence was almost negligible at fractions of PF 1–1 and PF 1–2 (Table 2). The instrumentation of UPLC-MS/MS is more sensitive to the qualitative determination of oligomers from both prodelphinidin (PD) and procyanidin (PC) type tannins. Overall prodelphinidin (PD) and procyanidin (PC) form of tannin were both identified for its presence at willow bark crude extracts by NMR and UPLC-MS/MS. The relative ratio of PC/PD was roughly 2.5 for crude extracts and PF0 at Table 2**,** and it was supported by the integral ratio (i.e. 2.3) between PC form and PD form from Fig. 4 and Fig. 5. The mDP was the highest from the crude extracts and dropped roughly 1.5 times to the

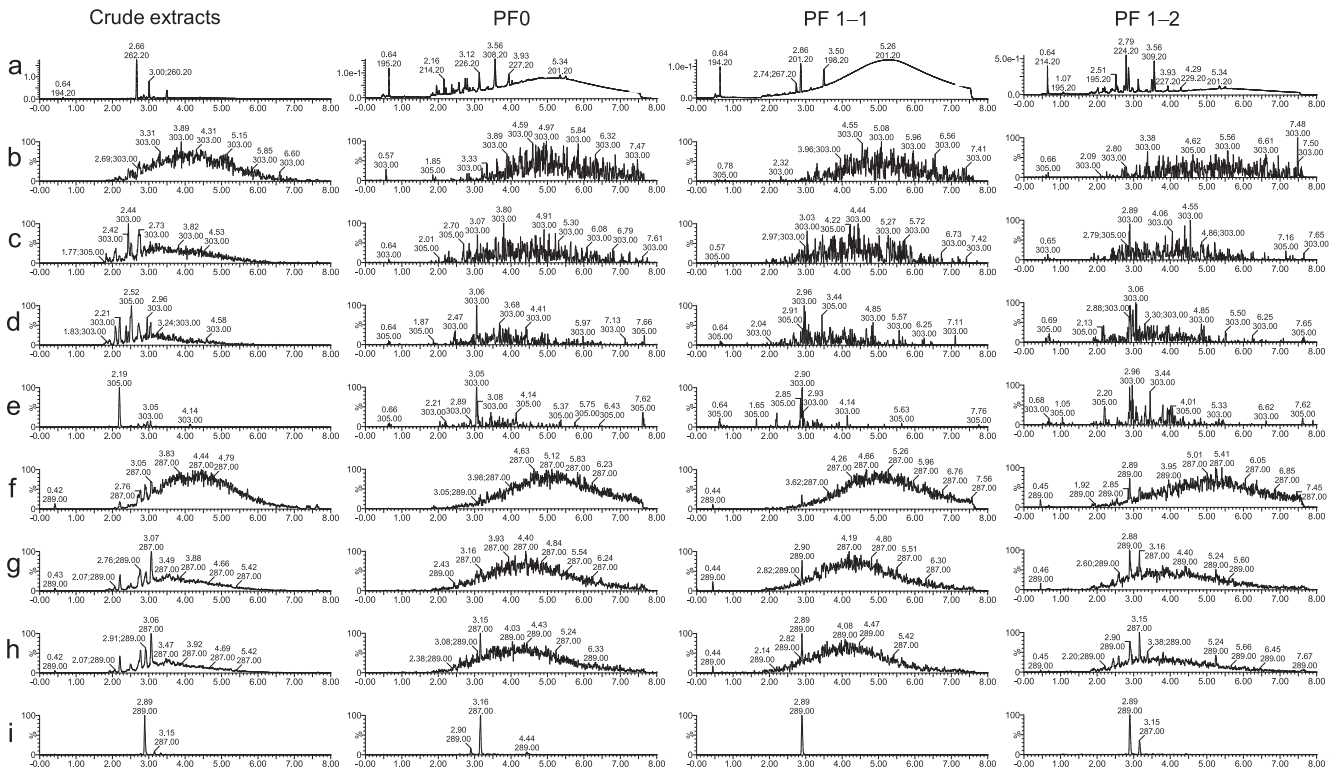

Fig. 6. UHPLC chromatograms of Karin bark crude extracts and its purified fractions (PF0; PF 1–1; and PF 1–2). a UHPLC-DAD chromatogram at 280 nm. b-d UHPLC-MS/MS chromatograms of prodelphinidin oligomers and polymers. e UHPLC-MS/MS chromatograms of gallocatechin and epigallocatechin monomers. f-h UHPLC-MS/MS chromatograms of procyanidin oligomers and polymers. i UHPLC-MS/MS chromatograms of catechin and epicatechin monomers.

Table 2
UPLC-MS/MS analysis results of Karin bark crude extracts and its purified fractions (PF0; PF 1–1; and PF 1–2).

	Total proanthocyanidins mg/g			
	PC	PD	Sum	mDP
Crude extracts	58.8	23	81.8	5.0
PF0	49	19.8	68.8	2.9
PF 1–1	10.6	1	11.6	3.2
PF 1–2	9.7	0.7	10.4	1.9

purified fractions, indicating that the purified fraction was also highly representative of the proanthocyanidins. Both the UPLC-MS/MS (Table 2) and size exclusion chromatography (SEC) (**Table S4**) suggest that the crude extracts have an average oligomerization degree of roughly 5–6 flavan-3-ol units.

3.4. Adsorption performance of activated foams (or foams) from crude extracts

The structural foundation (or characterization) of crude extracts provides a more rational design to apply this activated foam made of willow bark-derived proanthocyanidins as promising bio-based adsorbents for possible water treatment. Considering the potential applicability for the industrial wastewater treatment, crude extracts from two willow hybrids (Karin and Klara) were included for the water treatment experiments by using model solutions. Willow bark crude extracts (including hybrids Karin and Klara) were chemically foamed and further activated with steam treatment. They were then used as adsorbents in initial experiments for removing zinc (Zn^{2+}) and Bisphenol A (BPA). The specific surface area and porous morphology of the activated foam was achieved using the nitrogen sorption, as shown at Fig. 7. Interestingly, the mesoporous structure appears after the activation (with the yield of roughly 38%, Table 3), as reflected by the surface characteristics like specific surface area and pore volumes (micropores, mesopores, and macropores).

The surface acidity and porosity structure of the adsorbents are important aspects regarding the adsorption on the removal of zinc and BPA, respectively. As indicated in Table 3, the raw materials, Klara and Karin bark, did not remove BPA or zinc at all. The foams and especially the activated foams have a sponge-like structure with a large surface area. Foams (Ka-F and Kl-F) removed considerable amount of BPA but very low amount of zinc. Interestingly, activated foam samples (Ka-A-F and Kl-A-F) removed significantly both zinc and BPA for both willow hybrids. In specific, adsorption capacities of 9.19 mg/g (91 % removal efficiency) and 7.96 mg/g (79 % removal efficiency) were reported towards zinc removal for Ka-A-F and Kl-A-F, respectively. Interestingly, 100 % of initial BPA from the solution could be removed using activated foams (Ka-A-F and Kl-A-F) and can also be reported as having an adsorption capacity of 9.18 mg/g. In addition, the willow bark was carbonized previously as electrode materials. The adsorption capacities shown here from the crude extracts, representing 20 (w/w %) of Karin bark, maybe partly explain the hierarchically organized pore structure of the obtained electrode from willow bark as an energy storage system. [43] Overall there is clear established correlation between the surface area and the adsorption capacities in this study, as reported also previously. [44] Biomass-derived carbon materials have been used as an adsorbent earlier and results presented in literature showed huge variety towards the removal of BPA and zinc as seen in Table 4. Results obtained in this study was compared to the studies in which quite simple production step was used in the context of lignocellulosic biomass-derived material. Even though the screening adsorption experiments are currently only conducted by screening rather than under optimal conditions, the adsorption capacity has been proven to be in the same order of magnitude than the results presented in literature. Therefore, the willow bark crude extracts are of high importance comparing to the

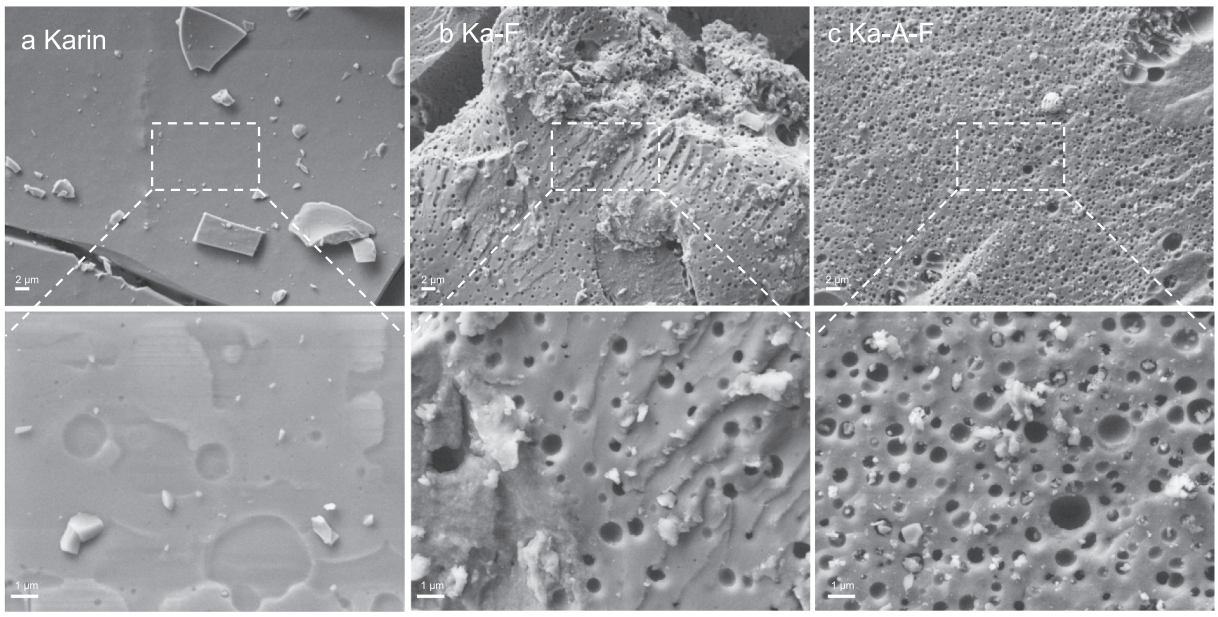

Fig. 7. Morphology of the prepared foam and activated foam from Karin bark crude extracts by FESEM imaging analysis. a Karin bark crude extracts. b Foam of crude extracts (Ka-F). c Activated foam of crude extracts (Ka-A-F). For Klara bark, see **Fig. S7**.

Table 3
Surface characteristics and adsorption capacities towards zinc and Bisphenol A (BPA) for the studied adsorbents. "a" denotes that the adsorption capacities for crude extracts was zero. Standard deviations are included inside the parenthesis.

		Unit	Ka-F	Ka-A-F	Kl-F	Kl-A-F
Specific surface area, pore volume, and pore size distribution	SSA (specific surface area)	m^2/g	0.3	734	0.02	717
	Total pore volume	cm^3/g	*	0.3	*	0.3
	Micropores < 2.2 nm	cm^3/g	*	0.3	*	0.3
	Mesopores 2.2–50 nm	cm^3/g	*	0.04	*	0.02
	Macropores > 50 nm	cm^3/g	*	0.002	*	0.001
	Micropores < 2.2 nm	%	*	86	*	92
	Mesopores 2.2–50 nm	%	*	13	*	8
	Macropores > 50 nm	%	*	1	*	0.4
	Yield after activation based on crude foam	%	–	39	–	37
Adsorption capacities[a]	q (zinc)	mg/g	0.99 ($6*10^{-2}$)	9.19 ($8*10^{-4}$)	0.88 (0.01)	7.96 (0.11)
	q (BPA)	mg/g	7.08 ($9.04*10^{-6}$)	9.18 (0)	6.33 ($7.1*10^{-6}$)	9.18 (0)

other bio-based materials.

4. Conclusion

The chemical composition of the proanthocyanidins fractions from crude extracts of willow bark has been determined using a novel analytical approach combining the use of both liquid (^{13}C and two-dimensional HSQC) and solid-state NMR spectroscopy. This NMR approaches offered information regarding the chemical structure of the elusive proanthocyanidins from crude extracts and its purified colorant fractions. To be specific, solid-state NMR provided generalized characteristic resonances of the overlapped procyanidins (PCs) and prodelphinidins (PDs) units of proanthocyanidin (PA) fractions from purified colorants and crude extracts. The flavan-3-ol unit showed clear and well-resolved absorbance regions in both ^{13}C and 2D HSQC NMR. Both the NMR and UPLC-MS/MS recognized both PCs and PDs units of proanthocyanidin from crude extracts and procyanidins units were identified as the main units present in the proanthocyanidins. The oligomeric nature of the crude extracts was also revealed by both the UPLC-MS/MS and SEC. Overall, the sensitivity of the applied technique towards the proanthocyanidin chemistry elucidation has been studied and this demonstrates the power of the concerted use of multiple techniques for the structural elucidation of bark-derived crude extracts. This study showed that the activated foam from willow bark crude extracts has the potential to be successfully applied to the industrial wastewater treatment.

In this study, only initial adsorption studies were implemented to test is the developed material showing adsorption capacity towards organics (BPA as model) or metals (Zn as model). Adsorption-regeneration cycles were not implemented and therefore, the detailed plan to optimize various parameters of adsorption and carry out ''long-term performance study'' using the willow bark-derived crude extracts (or its purified fractions) as adsorbent is out of scope of this present work and this will be investigated more carefully at another study.

Table 4
Comparison of adsorption capacity towards removal of organics (i.e. BPA) and heavy metals (i.e. zinc) between willow bark crude extracts (our study) and other lignocellulosic biomass-derived carbons.

Contaminant	Biomass	Preparation conditions	Adsorption capacity mg/g	Reference
Zinc	Almond shells	Physical activation by CO_2 at 850 °C	6.65	[45]
	Apricot stone	Physical activation with water vapour at 800 °C	13.21	[46]
	Birch sawdust	Physical activation with water vapour at 800 °C	21.44	[47]
	Valonia tannin resin	Treatment with NH_3 and formaldehyde, then HNO_3 at 80 °C	35.51	[4]
	Willow bark crude extracts	Carbonization at 800 °C	7.96–9.19	present study
Bisphenol A	Biomass-based carbon residue from gasification plant	Chemical activation with $FeCl_3$ at room temperature	41.5	[48]
	Moso bamboo (*Phyllostachys pubescens*)	Physical treatment at 400 °C	2.1	[49]
	Moso bamboo (*Phyllostachys pubescens*)	Physical treatment at 700 °C	11.4	[49]
	Wood chips	Carbonization at 800 °C	4.2–18.2	[50]
	Willow bark crude extracts	Carbonization at 800 °C	9.18	present study

CRediT authorship contribution statement

Dou Jinze: Conceptualization, Methodology, Resources, Project administration, Funding acquisition, Writing – original draft, Validation, Formal analysis, Writing – review & editing. **Varila Toni:** Validation, Formal analysis, Writing – review & editing. **Salminen Juha-Pekka:** Supervision, Writing – review & editing. **Tuomikoski Sari:** Validation, Formal analysis, Writing – review & editing. **Hietala Sami:** Validation, Formal analysis, Writing – review & editing. **Hemmi Maria:** Validation, Formal analysis, Writing – review & editing. **Hu Tao:** Validation, Formal analysis, Writing – review & editing. **Lassi Ulla:** Supervision, Writing – review & editing. **Vuorinen Tapani:** Supervision, Writing – review & editing.

Declaration of Competing Interest

The authors declare that they have no known competing financial interests or personal relationships that could have appeared to influence the work reported in this paper.

Acknowledgements

This work made use of the RawMatTERS Finland infrastructure (RAMI) facilities based at Aalto University. This work was a part of the Academy of Finland's Flagship Programme under Project No. 318890 and No. 318891 (Competence Center for Materials Bioeconomy, FinnCERES). Dr. Leena Pitkänen from Aalto University provided the assistance for the molecular weight analysis using Gel Permeation Chromatography. The NMR premises from the University of Helsinki is also appreciated.

Appendix A. Supplementary material

Supplementary data to this article can be found online at https://doi.org/10.1016/j.seppur.2023.123943.

References

[1] S. Lemonick, Looking for Finland's Future in Its Forests, ACS Cent. Sci. 4 (2018) 424–427, https://doi.org/10.1021/acscentsci.8b00202.
[2] Food and Agriculture Organization of the United Nations (2015) Forest products. In: FAO Forestry Series and FAO Statistics Series.
[3] M. Jablonsky, J. Nosalova, A. Sladkova, A. Haz, F. Kreps, J. Valka, S. Miertus, V. Frecer, M. Ondrejovic, J. Sima, I. Surina, Valorisation of softwood bark through extraction of utilizable chemicals. A review, Biotechnol. Adv. 35 (2017) 726–750, https://doi.org/10.1016/j.biotechadv.2017.07.007.
[4] R.K. Devappa, S.K. Rakshit, R.F.H. Dekker, Forest biorefinery: Potential of poplar phytochemicals as value-added co-products, Biotechnol. Adv. 33 (2015) 681–716, https://doi.org/10.1016/j.biotechadv.2015.02.012.
[5] J.P. Salminen, M. Karonen, Chemical ecology of tannins and other phenolics: we need a change in approach, Funct. Ecol. 25 (2011) 325–338, https://doi.org/10.1111/j.1365-2435.2010.01826.x.
[6] J.P. Salminen, Two-Dimensional Tannin Fingerprints by Liquid Chromatography Tandem Mass Spectrometry Offer a New Dimension to Plant Tannin Analyses and Help To Visualize the Tannin Diversity in Plants, J. Agric. Food Chem. 66 (2018) 9162–9171, https://doi.org/10.1021/acs.jafc.8b02115.
[7] A. Bello, U. Bergmann, J. Vepsäläinen, T. Leiviskä, Effects of tree harvesting time and tannin cold/hot-water extraction procedures on the performance of spruce tannin biocoagulant for water treatment, Chem. Eng. J. 449 (2022), 137809, https://doi.org/10.1016/j.cej.2022.137809.
[8] G. Palma, J. Freer, J. Baeza, Removal of metal ions by modified *Pinus radiata* bark and tannins from water solutions, Water Res. 37 (2003) 4974–4980, https://doi.org/10.1016/j.watres.2003.08.008.
[9] H.A.M. Bacelo, S.C.R. Santos, C.M.S. Botelho, Tannin-based biosorbents for environmental applications – A review, Chem. Eng. J. 303 (2016) 575–587, https://doi.org/10.1016/j.cej.2016.06.044.
[10] J.B. Neris, F.H.M. Luzardo, E.G.P. da Silva, F.G. Velasco, Evaluation of adsorption processes of metal ions in multi-element aqueous systems by lignocellulosic adsorbents applying different isotherms: A critical review, Chem. Eng. J. 357 (2019) 404–420, https://doi.org/10.1016/j.cej.2018.09.125.
[11] Y. Yazaki, Utilization of Flavonoid Compounds from Bark and Wood: A Review, Nat. Prod. Commun. 10 (2015) 513–520, https://doi.org/10.1177/1934578X1501000333.
[12] J. Hytönen, A. Saarsalmi, Long-term biomass production and nutrient uptake of birch, alder and willow plantations on cut-away peatland, Biomass Bioenergy 33 (2009) 1197–1211, https://doi.org/10.1016/j.biombioe.2009.05.014.
[13] H. Rosenqvist, A. Roos, E. Ling, B. Hektor, Willow growers in Sweden, Biomass Bioenergy 18 (2000) 137–145, https://doi.org/10.1016/s0961-9534(99)00081-1.
[14] J. Dou, W. Xu, J.J. Koivisto, J.K. Mobley, D. Padmakshan, M. Kögler, C. Xu, S. Willför, J. Ralph, T. Vuorinen, Characteristics of Hot Water Extracts from the Bark of Cultivated Willow (*Salix* sp.), ACS Sustainable Chem. Eng. 6 (2018) 5566–5573, https://doi.org/10.1021/acssuschemeng.8b00498.
[15] K.K. Kesari, A. Dhasmana, S. Shandilya, N. Prabhakar, A. Shaukat, J. Dou, J. M. Rosenholm, T. Vuorinen, J. Ruokolainen, Plant-Derived Natural Biomolecule Picein Attenuates Menadione Induced Oxidative Stress on Neuroblastoma Cell Mitochondria, Antioxidants 9 (2020) 552, https://doi.org/10.3390/antiox9060552.
[16] J. Dou, M. Rissanen, P. Ilina, H. Mäkkylä, P. Tammela, S. Haslinger, T. Vuorinen, Separation of fiber bundles from willow bark using sodium bicarbonate and their novel use in yarns for superior UV protection and antibacterial performance, Ind. Crops Prod. 164 (2021), 113387, https://doi.org/10.1016/j.indcrop.2021.113387.
[17] J. Dou, L. Galvis, U. Holopainen-Mantila, M. Reza, T. Tamminen, T. Vuorinen, Morphology and Overall Chemical Characterization of Willow (*Salix* sp.) Inner Bark and Wood: Toward Controlled Deconstruction of Willow Biomass, ACS Sustainable, Chem. Eng. 4 (2016) 3871–3876, https://doi.org/10.1021/acssuschemeng.6b00641.
[18] J. Dou, V. Chandgude, T. Vuorinen, S. Bankar, S. Hietala, H.Q. Lê, Enhancing Biobutanol Production from biomass willow by pre-removal of water extracts or bark, J. Cleaner Prod. 327 (2021), 129432, https://doi.org/10.1016/j.jclepro.2021.129432.
[19] H.M. Zwain, M. Vakili, I. Dahlan, Waste Material Adsorbents for Zinc Removal from Wastewater: A Comprehensive Review, Int. J. Chem. Eng. 2014 (2014), 347912, https://doi.org/10.1155/2014/347912.
[20] H. Melcer, G. Klečka, Treatment of wastewaters Containing Bisphenol A: State of the Science Review, Water Environ. Res. 83 (2011) 650–666, https://doi.org/10.2175/106143010X12851009156925.
[21] P. Guerra, M. Kim, S. Teslic, M. Alaee, S.A. Smyth, Bisphenol-A removal in various wastewater treatment processes: operational conditions, mass balance, and optimization, J. Environ. Manage. 152 (2015) 192–200, https://doi.org/10.1016/j.jenvman.2015.01.044.
[22] N.A.A. Qasem, R.H. Mohammed, D.U. Lawal, Removal of heavy metal ions from wastewater: a comprehensive and critical review. npj Clean, Water 4 (2021) 36, https://doi.org/10.1038/s41545-021-00127-0.
[23] J. Dou, J. Heinonen, T. Vuorinen, C. Xu, T. Sainio, Chromatographic recovery and purification of natural phytochemicals from underappreciated willow bark water

extracts, Sep. Purif. Technol. 261 (2021), 118247, https://doi.org/10.1016/j.seppur.2020.118247.
[24] S. Agnolet, S. Wiese, R. Verpoorte, D. Staerk, Comprehensive analysis of commercial willow bark extracts by new technology platform: Combined use of metabolomics, high-performance liquid chromatography–solid-phase extraction–nuclear magnetic resonance spectroscopy and high-resolution radical scavenging assay, J. Chromatogr. A 1262 (2012) 130–137, https://doi.org/10.1016/j.chroma.2012.09.013.
[25] L. Pobłocka-Olech, A.M. van Nederkassel, Y.V. Heyden, M. Krauze-Baranowska, D. Glód, T. Baczek, Chromatographic analysis of salicylic compounds in different species of the genus *Salix*, J. Sep. Sci. 30 (2007) 2958–2966, https://doi.org/10.1002/jssc.200700137.
[26] S. Brunauer, P.H. Emmett, E. Teller, Adsorption of gases in multimolecular layers, J. Am. Chem. Soc. 60 (1938) 309–319, https://doi.org/10.1021/ja01269a023.
[27] N.A. Seaton, J.P.R.B. Walton, N. Quirke, A new analysis method for the determination of the pore size distribution of porous carbons from nitrogen adsorption measurements, Carbon 27 (1989) 853–861, https://doi.org/10.1016/0008-6223(89)90035-3.
[28] C. Lastoskie, K.E. Gubbins, N. Quirke, Pore size distribution analysis of microporous carbons: a density functional theory approach, J. Phys. Chem. 97 (1993) 4786–4796, https://doi.org/10.1021/j100120a035.
[29] V.A. Hackley, A.B. Stefaniak, "Real-world" precision, bias, and between-laboratory variation for surface area measurement of a titanium dioxide nanomaterial in powder form, J. Nanopart. Res. 15 (2013) 1742, https://doi.org/10.1007/s11051-013-1742-y.
[30] M.A. Zarin, H.Y. Wan, A. Isha, N. Armania, Antioxidant, antimicrobial and cytotoxic potential of condensed tannins from *Leucaena leucocephala* hybrid-Rendang, Food Sci. Hum. Wellness 5 (2016) 65–75, https://doi.org/10.1016/j.fshw.2016.02.001.
[31] J. Dou, A. Karakoç, L.S. Johansson, S. Hietala, D. Evtyugin, T. Vuorinen, Mild alkaline separation of fiber bundles from eucalyptus bark and their composites with cellulose acetate butyrate, Ind. Crops Prod. 165 (2021), 113436, https://doi.org/10.1016/j.indcrop.2021.113436.
[32] C.S. Malisch, A. Lüscher, N. Baert, M.T. Engström, B. Studer, C. Fryganas, D. Suter, I. Mueller-Harvey, J.P. Salminen, Large Variability of Proanthocyanidin Content and Composition in Sainfoin *(Onobrychis viciifolia*), J. Agric. Food Chem. 63 (2015) 10234–10242, https://doi.org/10.1021/acs.jafc.5b04946.
[33] M.T. Engström, M. Pälijärvi, C. Fryganas, J.H. Grabber, I. Mueller-Harvey, J. P. Salminen, Rapid Qualitative and Quantitative Analyses of Proanthocyanidin Oligomers and Polymers by UPLC-MS/MS, J. Agric. Food Chem. 62 (2014) 3390–3399, https://doi.org/10.1021/jf500745y.
[34] J. Dou, P. Ilina, J. Hemming, K. Malinen, H. Mäkkylä, N.O. de Farias, P. Tammela, G.D.A. Umbuzeiro, R. Räisänen, T. Vuorinen, Effect of Hybrid Type and Harvesting Season on Phytochemistry and Antibacterial Activity of Extracted Metabolites from *Salix* Bark, J. Agric. Food Chem. 70 (2022) 2948–2956, https://doi.org/10.1021/acs.jafc.1c08161.
[35] Y.B. Hoong, A. Pizzi, P.M. Tahir, H. Pasch, Characterization of *Acacia mangium* polyflavonoid tannins by MALDI-TOF mass spectrometry and CP-MAS ^{13}C NMR, Eur. Polym. J. 46 (2010) 1268–1277, https://doi.org/10.1016/j.eurpolymj.2010.03.002.
[36] G. Jürgenliemk, F. Petereit, A. Nahrstedt, Flavan-3-ols and procyanidins from the bark of *Salix purpurea* L, Pharmazie 62 (2007) 231–234.
[37] C. Fryganas, C. Drake, H.M. Ropiak, M. Mora-Ortiz, L.M.J. Smith, I. Mueller-Harvey, R.M. Kowalczyk, Carbon-13 Cross-Polarization Magic-Angle Spinning Nuclear Magnetic Resonance for Measuring Proanthocyanidin Content and Procyanidin to Prodelphinidin Ratio in Sainfoin *(Onobrychis viciifolia*) Tissues, J. Agric. Food Chem. 66 (2018) 4073–4081, https://doi.org/10.1021/acs.jafc.8b01215.
[38] D.G. Reid, S.L. Bonnet, G. Kemp, J.H. van der Westhuizen, Analysis of commercial proanthocyanidins. Part 4: Solid state ^{13}C NMR as a tool for *in situ* analysis of proanthocyanidin tannins, in heartwood and bark of quebracho and acacia, and related species, Phytochemistry 94 (2013) 243–248, https://doi.org/10.1016/j.phytochem.2013.06.007.
[39] P.N. Diouf, C.M. Tibirna, M. García-Pérez, M. Royer, P. Dubé, T. Stevanovic, Structural Elucidation of Condensed Tannin from *Picea mariana* Bark, J. Biomater. Nanobiotechnol. 4 (2013) 1–8, https://doi.org/10.4236/jbnb.2013.43A001.
[40] A. Duval, L. Avérous, Characterization and Physicochemical Properties of Condensed Tannins from *Acacia catechu*, J. Agric. Food Chem. 64 (2016) 1751–1760, https://doi.org/10.1021/acs.jafc.5b05671.
[41] W.E. Zeller, A. Ramsay, H.M. Ropiak, C. Fryganas, I. Mueller-Harvey, R.H. Brown, C. Drake, J.H. Grabber, ^{1}H–^{13}C HSQC NMR Spectroscopy for Estimating Procyanidin/ Prodelphinidin and *cis/trans*-Flavan-3-ol Ratios of Condensed Tannin Samples: Correlation with Thiolysis, J. Agric. Food Chem. 63 (2015) 1967–1973, https://doi.org/10.1021/jf504743b.
[42] C. Crestini, H. Lange, G. Bianchetti, Detailed Chemical Composition of Condensed Tannins via Quantitative ^{31}P NMR and HSQC Analyses: *Acacia catechu, Schinopsis balansae*, and *Acacia mearnsii*, J. Nat. Prod. 79 (2016) 2287–2295, https://doi.org/10.1021/acs.jnatprod.6b00380.
[43] M.A. Hobisch, J. Phiri, J. Dou, P. Gane, T. Vuorinen, W. Bauer, C. Prehal, T. Maloney, S. Spirk, Willow Bark for Sustainable Energy Storage Systems, Materials 13 (2020) 1016, https://doi.org/10.3390/ma13041016.
[44] T. Otowa, R. Tanibata, M. Itoh, Production and adsorption characteristics of MAXSORB: High-surface-area active carbon, Gas Sep. Purif. 7 (1993) 241–245, https://doi.org/10.1016/0950-4214(93)80024-Q.
[45] M.A. Ferro-García, J. Rivera-Utrilla, J. Rodríguez-Gordillo, I. Bautista-Toledo, Adsorption of zinc, cadmium, and copper on activated carbons obtained from agricultural by-products, Carbon 26 (1988) 363–373, https://doi.org/10.1016/0008-6223(88)90228-X.
[46] T.K. Budinova, N.V. Petrov, V.N. Minkova, K.M. Gergova, Removal of metal ions from aqueous solution by activated carbons obtained from different raw materials, J. Chem. Technol. Biotechnol. 60 (1994) 177–182, https://doi.org/10.1002/jctb.280600210.
[47] S. Tuomikoski, R. Kupila, H. Romar, D. Bergna, T. Kangas, H. Runtti, U. Lassi, Zinc Adsorption by Activated Carbon Prepared from Lignocellulosic Waste Biomass, Appl. Sci. 9 (2019) 4583, https://doi.org/10.3390/app9214583.
[48] R. Juhola, H. Runtti, T. Kangas, T. Hu, H. Romar, S. Tuomikoski, Bisphenol A removal from water by biomass-based carbon: isotherms, kinetics and thermodynamics studies, Environ. Technol. 41 (2020) 971–980, https://doi.org/10.1080/09593330.2018.1515990.
[49] T. Asada, K. Oikawa, K. Kawata, S. Ishihara, T. Iyobe, A. Yamada, Study of Removal Effect of Bisphenol A and *β*-Estradiol by Porous Carbon, J. Health Sci. 50 (2004) 588–593, https://doi.org/10.1248/jhs.50.588.
[50] A. Nakanishi, M. Tamai, N. Kawasaki, T. Nakamura, S. Tanada, Adsorption Characteristics of Bisphenol A onto Carbonaceous Materials Produced from Wood Chips as Organic Waste, J. Colloid Interface Sci. 252 (2002) 393–396, https://doi.org/10.1006/jcis.2002.8387.